Deciphering Structures of Inclusion Complexes of Amylose with Natural Phenolic Amphiphiles

Kumar, Kamlesh; Loos, Katja

Published in:
ACS Omega

DOI:
10.1021/acsomega.9b02388

Publication date:
2019

ACS OMEGA

Article

Cite This: ACS Omega 2019, 4, 17807−17813

http://pubs.acs.org/journal/acsodf

Deciphering Structures of Inclusion Complexes of Amylose with Natural Phenolic Amphiphiles

Kamlesh Kumar*,# and Katja Loos*

Macromolecular Chemistry and New Polymeric Materials, Zernike Institute for Advanced Materials, University of Groningen, Nijenborgh 4, 9747 AG Groningen, The Netherlands

ABSTRACT: Amylose inclusion complexes were prepared in aqueous solution with the amphiphilic moiety 3-pentadecylphenol via a direct mixing method. Attenuated total reflection Fourier transform infrared spectroscopy as well as differential scanning calorimetry confirmed the formation of amylose inclusion complexes. The morphology of the synthesized complexes is sensitive to temperature, and X-ray data revealed that the inclusion complexes exhibited distinct structures at different temperatures. Small-angle X-ray scattering data indicated ordered lamellar structures of the synthesized complexes at room temperature, and wide-angle X-ray scattering profiles showed the transformation of the crystalline structure as a function of the temperature. The results of this research will help to understand the relationship between the inclusion complex structures with temperature.

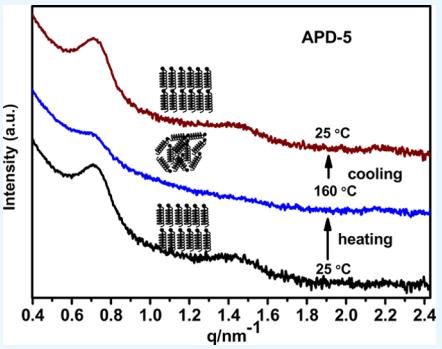

1. INTRODUCTION

Starch is composed of two distinct components: essentially linear or slightly branched amylose consisting of α-1,4-glycosidic bonds and highly branched amylopectin having α-1,4-glycosidic and α-1,6-glycosidic bonds.[1−3] The amylose chains have a helical hydrophobic interior cavity, and it is known to form inclusion complexes via hydrophobic−hydrophobic interactions[4−8] with hydrophobic guest moieties such as dyes,[9] flavors,[10,11] lactones,[12] polymers,[13−15] and lipids.[16,17] The formation of the complex increases the physical and chemical stability of lipophilic guest molecules by shielding them against oxidation, evaporation, and decomposition. These kinds of inclusion complexes show their potential applications in food and pharmaceutical applications for nanoencapsulation,[18] control release of the drugs,[19] and flavor encapsulations.[20]

Different ligands display a distinct interaction with amylose, and their interactions can significantly influence the structural properties of amylose inclusion complexes. The morphologies of the amylose inclusion complexes are known to be greatly affected by experimental conditions such as concentration of amylose and guest molecules, temperature, and pressure.[7a,11] Depending on the guest molecules, amylose inclusion complexes of 6, 7, or 8 glucosyl residues per helical turn are obtained for alcohols, acetone, lipids, and naphthol.[21−23] Therefore, it is always interesting to explore distinct crystal structures of the resulting complexes of amylose with different complexing agents.

The impact of guest molecules and other experimental parameters on the morphological properties of synthesized inclusion complexes are most often explored by X-ray scattering techniques, and we have recently explored the structural characterization of amylose-polymer inclusion complexes by these techniques.[6,7] In the present study, different concentrations of the pentadecylphenol (PDP) complexing agent is used to form amylose-PDP inclusion complexes. PDP is a naturally occurring amphiphilic phenolic surfactant obtained from cashew nut oils and has potential applications in medicine, resin additives, and fuel additives.[24] Facilitating the formation of inclusion complexes with phenolic surfactants can extend the shelf life of food products via reducing enzymatic browning.

The objective of this work was to synthesize inclusion complexes of amylose with PDP and to further systematically elucidate the morphological characteristics via attenuated total reflection Fourier transform infrared spectroscopy (ATR-FTIR), wide-angle X-ray scattering (WAXS), and small-angle X-ray scattering (SAXS) characterization techniques. The effects of temperature and guest molecule concentration on the morphology of amylose-PDP inclusion complex were also investigated.

2. EXPERIMENTAL SECTION

2.1. Materials. Amylose with a molecular weight of ∼ 180 kg/mol was received from Avebe. PDP was purchased from Sigma-Aldrich. PDP was recrystallized from petroleum ether and dried under vacuum at room temperature for 24 h.

2.2. Synthesis of Amylose-PDP Inclusion Complexes. Amylose-PDP complexes were prepared by suspending 500 mg of amylose in 15 mL of deionized water followed by mixing 5, 10, and 20% (w/w) PDP. The solution was rotated at room temperature for 2 h and transferred to a pressure vessel. The pressure vessel was heated to 160 °C for 1 h followed by cooling down to 80 °C. The solution was continuously rotated at 80 °C overnight. Thereafter, the solutions were cooled down to room

Received: July 29, 2019
Accepted: October 2, 2019
Published: October 17, 2019

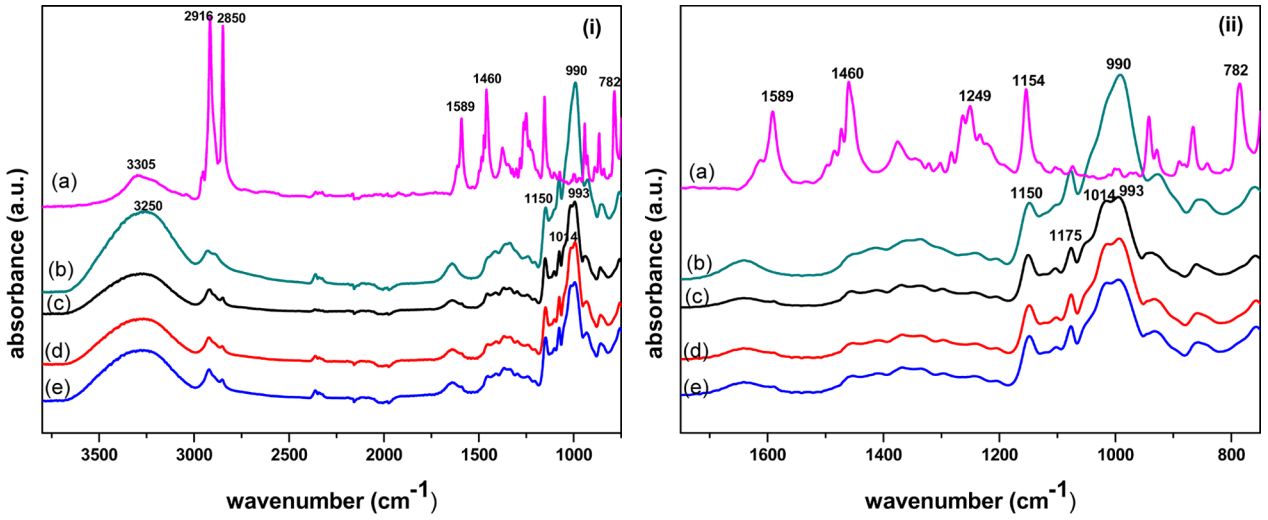

Figure 1. ATR-FTIR spectra of (a) PDP, (b) amylose, (c) APD-5, (d) APD-10, and (e) APD-20. (i) Wavenumber range 750 to 3800 cm^{-1}. (ii) Magnified range of panel (i) between 750 and 1750 cm^{-1}.

temperature and centrifuged at 2500 rpm for 30 min. The supernatants were discarded, and filtrates were washed with hot water to remove noncomplexed PDP. The washed precipitate samples were freeze-dried overnight. The complexes of amylose with PDP mass ratios of 20:1, 10:1, and 5:1 are presented as APD-5, APD-10, and APD-20, respectively.

2.3. Characterization. Fourier transform infrared spectra were recorded by a Bruker IFS88 FT-IR spectrometer equipped with n MCT-A detector at a resolution of 4 cm^{-1}. The simultaneous measurements of WAXS and SAXS data as a function of temperature were measured at the Dutch-Belgium Beamline (DUBBLE) station BM26B of the European Synchrotron Radiation Facility (ESRF) in Grenoble, France. The sample to detector distance of the SAXS setup was ~3.5 m, and the X-ray wavelength was 1.03 Å. A Linkam DSC 600 cell was used to execute temperature resolved measurements. The X-ray patterns were recorded with a heating/cooling rate of 5 °C/min in the temperature range of 25 to 160 °C. The scattering vector q is denoted here as $q = 4\pi/\lambda(\sin\theta)$, where 2θ is the scattering angle.[25]

3. RESULTS AND DISCUSSION

Three different compositions of PDP molecules were mixed with amylose to form inclusion complexes. The chemical structures of the pristine materials and conformational changes during the complex formation were investigated by FTIR. The FTIR spectra of PDP (a), amylose (b), and different compositions (20:1, 10:1, and 5:1 mass ratios) of amylose guest molecule (c), (d), and (e) are presented in Figure 1.

The common functional group stretching and bending vibrations of the amylose appeared in the range of 900−1200 and 2800−3400 cm^{-1}, respectively. The typical characteristic peaks of the C−C and C−O bonds of amylose were positioned at about 990, 1080, and 1150 cm^{-1}. The stretching vibration of the C−O−C glycosidic bond and O−H bonds were displayed at 850 and 3250 cm^{-1}, respectively (Figure 1b).[26−28] The FTIR spectrum of PDP showed a broad absorption band of the phenolic hydroxyl group at 3305 cm^{-1}. The absorption bands of the long pentadecyl chain were centered at 2916 and 2850 cm^{-1}. The characteristic peaks of the substituted aromatic ring were found at 1589, 1460, and 782 cm^{-1} (Figure 1a).[29]

Typically, the FTIR spectra of amylose-PDP inclusion complexes (Figure 1c,d) exhibited the vibrational peaks of amylose and PDP. However, due to the insertion of PDP into the amylose cavity, several characteristic absorption peaks of PDP between 1600 and 1000 almost vanished in the inclusion complex spectra. Moreover, the inclusion of the guest molecule splits the band of 990 cm^{-1} into two separate peaks, and these peaks appeared at 993 and 1014 cm^{-1} in the inclusion complex spectra.[7] The intensities of these peaks decreased with increasing concentration of the PDP guest molecules.

The amylose characteristic peaks at 1640, 1080, and 855 cm^{-1} were found to shift at 1645, 1076, and 860 cm^{-1}, respectively. The shifting of the vibrational frequencies is similar to the shifts reported elsewhere for amylose inclusion complex systems.[7,30] The intensity of the peak at 2850 cm^{-1} increased with the insertion of PDP inside the amylose cavity. Moreover, the broadening of the −OH peak at around 3280 cm^{-1} occurred in the complex. The disappearance of the guest absorption peaks, splitting of the 990 cm^{-1} band, and broadening of the −OH peak in the complex spectrum confirmed the formation of the amylose-PDP inclusion complex. Furthermore, the FTIR results suggest that the hydrophobic forces are responsible for transfer of the PDP molecule into the hydrophobic amylose helix cavity to form the amylose-PDP inclusion complex.[31]

The thermal properties of the amylose and inclusion complexes were characterized by differential scanning calorimetry (DSC) (Figure 2). The thermogram of amylose-PDP inclusion complexes showed an endotherm as compared to pristine amylose that arises due to dissociation of the inclusion complexes. A more detailed description of this behavior can be found elsewhere.[7,31,32] By increasing the concentration of PDP, the endotherm enthalpy peak of the inclusion complexes sharpens due to the higher crystalline nature of PDP. Furthermore, the endothermic enthalpy increased with the concentration of PDP molecules, which proved to be better complexation between amylose and PDP at higher concentrations.

The effects of thermal treatment and concentration of PDP on inclusion complex structures were analyzed using synchrotron X-ray measurement. The SAXS patterns of the APD-5 and APD-20 inclusion complexes were recorded as a function of

DOI: 10.1021/acsomega.9b02388
ACS Omega 2019, 4, 17807−17813

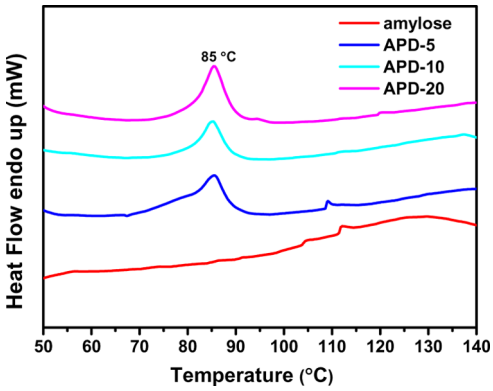

Figure 2. Thermograms (heating scan) of amylose and inclusion complexes between amylose and three different concentrations of PDP (ADP-5, APD-10, and APD-20).

temperature (25 to 160 °C and vice versa) as shown in Figures 3 and 4, respectively.

The scattering peaks at q of 0.7, 1.4, and 2.1 nm^{-1} suggested a lamellar structure of the amylose-PDP inclusion complexes at room temperature.[33] Biais et al. reported that the lamellar structural organization of the amylose complex constituted by alternating crystalline and amorphous layers.[34] The starting peak at 0.7 nm^{-1} is associated with the thickness of this lamellar morphology.[35]

The van der Waals forces, mainly hydrophobic−hydrophobic interactions and H-bonds, play an important role in the inclusion complex formation. The strength of Van der Waals forces decreased with increasing temperature, and it had a significant influence on the inclusion complex morphology. It was observed that the inclusion complexes started to dissociate at 70 °C that is above the melting temperature of PDP (54 °C), and this is indicated by a reduction in the ordering of the lamellar structure. Furthermore, the SAXS patterns showed that the intensity of peaks decreased with increasing temperature and less well-defined peaks were obtained at the higher temperature. The cooling X-ray profile showed the reorder of the lamellar structure of the inclusion complexes. SAXS revealed the lamellar morphology and disruption of the ordered lamellar morphology of the amylose-PDP complexes with the temperature.

The concentrations of amylose and complexing agent have a significant impact on the morphology of the complexes. It was reported that the concentration of the complexing agents can induce more than one type of crystalline structure.[36,37]

In the present study, the influence of the complexing agent concentration on the inclusion complexes was investigated, and SAXS diagrams of a higher amount of PDP (20 wt %) are recorded as a function of temperature. The heating and cooling cycles of the inclusion complex are presented in Figure 4a,b, respectively. As shown in Figure 4a, APD-20 showed two characteristic peaks at about 0.7 and 1.4 nm^{-1}, which confirms a

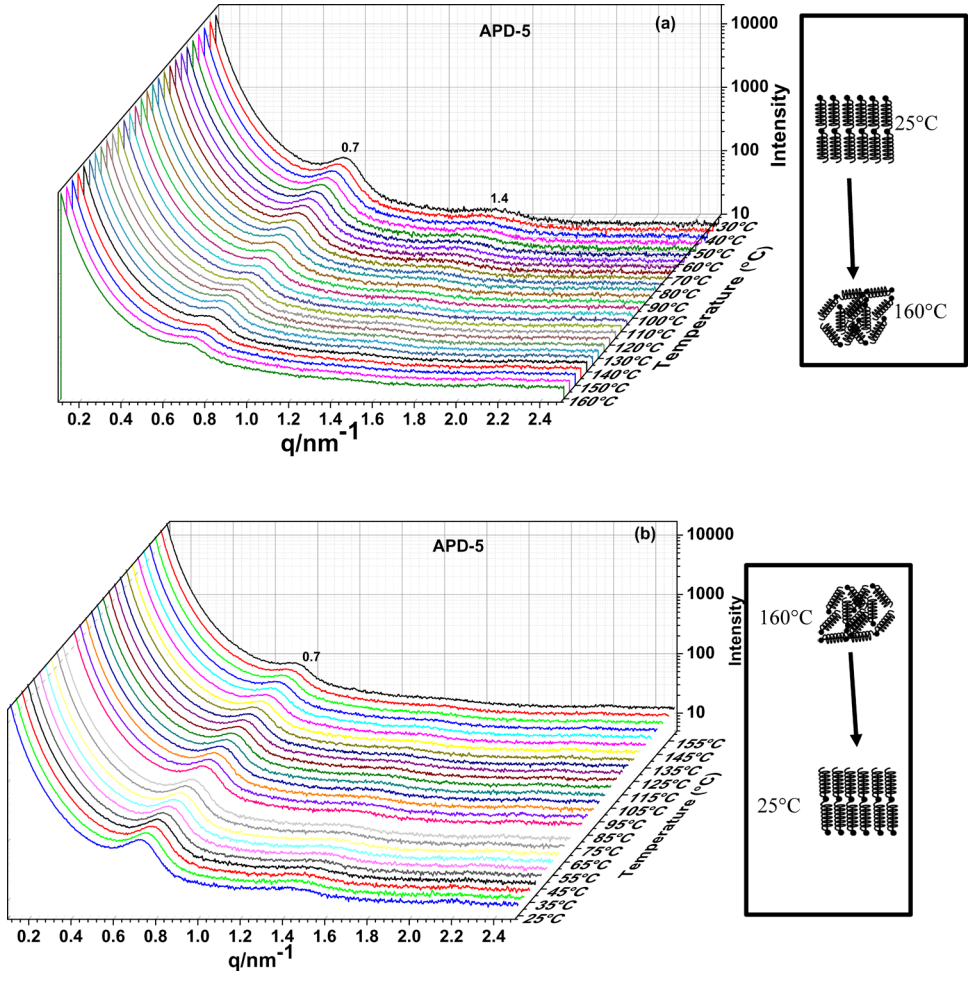

Figure 3. SAXS intensity profiles from APD-5 inclusion complex during (a) heating cycle (b) cooling cycle.

DOI: 10.1021/acsomega.9b02388
ACS Omega 2019, 4, 17807−17813

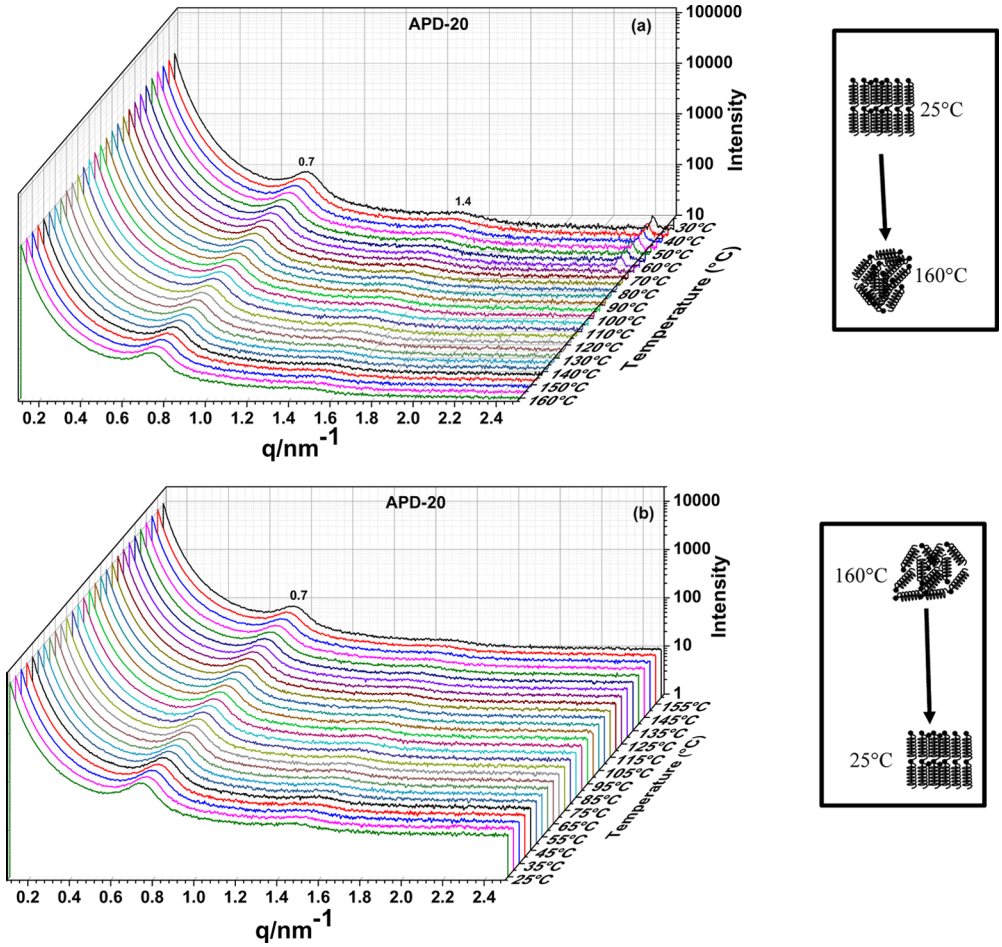

Figure 4. SAXS patterns of APD-20 during (a) heating cycle and (b) cooling cycle.

lamellar structure of the inclusion complex. However, higher PDP concentration reduced the intensity of the higher order peaks. These results indicated that increasing the amount of complexing agent might induce the random arrangements of well-defined domains of alternating layers of crystalline and amorphous regions.

The inclusion complexes were heated up to about 160 °C to redissolve the complexes followed by cooling back to room temperature to allow recrystallization of the complexes. The crystalline structure of the inclusion complexes during the heat treatment was investigated by WAXS. The representative WAXS patterns of the APD-5 and APD-20 complexes as a function of temperature are shown in Figure 5. As shown in Figure 5a, the diffraction patterns exhibit a typical crystalline structure displayed by different peaks at 10.7, 12.5, 12.8, 13.5, 14.0, 15.8, and 17.1 nm^{-1} at 25 °C.[38−40] After heat treatment, the intensities of the peaks changed and shifted to new positions at 11.5, 12.8, 14.5, and 17.4 nm^{-1}.

The transition to a different crystalline structure with temperature can be explained by temperature of crystallization and stabilizing the guest molecule in the hydrophobic cavity of the amylose molecules.[41] The WAXS data demonstrated that the inclusion complex crystallizes into two polymorphs with the temperature. Similar transformations of the crystalline structure of amylose inclusion complexes during heat treatment have also been reported elsewhere.[42,43] The complexes showed a stable crystal structures after the heat treatment, and it remains intact during cooling as well. Furthermore, a dominated sharp peak at 12.8 nm^{-1} of the heat-treated sample suggested that the higher temperature induced the crystalline size of the complex.

The WAXS profile of APD-20 at room temperature (Figure 5c,d) displays more vivid peaks as compared to APD-5, and these peaks are located at 8.7, 10.7, 12.4, 12.8, 13.5, 14.0, 17.0 nm^{-1}. It is observed that the reorganization of less perfect crystalline structures occurred with the temperature via restructuring of amorphous and crystalline lamellae in order to provide more impeccable crystalline structures.[44−46] The increasing number of peaks indicates that regularity of the inclusion complex increased with the amount of crystalline host molecules.[47] Similar to APD-5, the peaks moved to new positions at 8.5, 9.2, 11.6, 12.9, and 17.5 nm^{-1} after the heat treatment, which confirmed the transformations of the crystalline structure of the complex due to the heat treatment.[42,43] Some variations in the diffracted intensity of the peak at 12.9 cm^{-1} was observed with different concentrations of complexing agents due to different crystal sizes of the complex. Figure 6 displays SAXS and WAXS patterns at room temperature of APD-5, APD-10, and APD-20. The SAXS profile clearly shows the presence of lamellar patterns of the peaks.

4. CONCLUSIONS

The results of this study prove that PDP can be effectively inserted into the hydrophobic cavity of amylose in order to form amylose-PDP inclusion complexes. The formation of the inclusion complexes was confirmed by FTIR and DSC measurements. The DSC thermograms revealed an increased

DOI: 10.1021/acsomega.9b02388
ACS Omega 2019, 4, 17807−17813

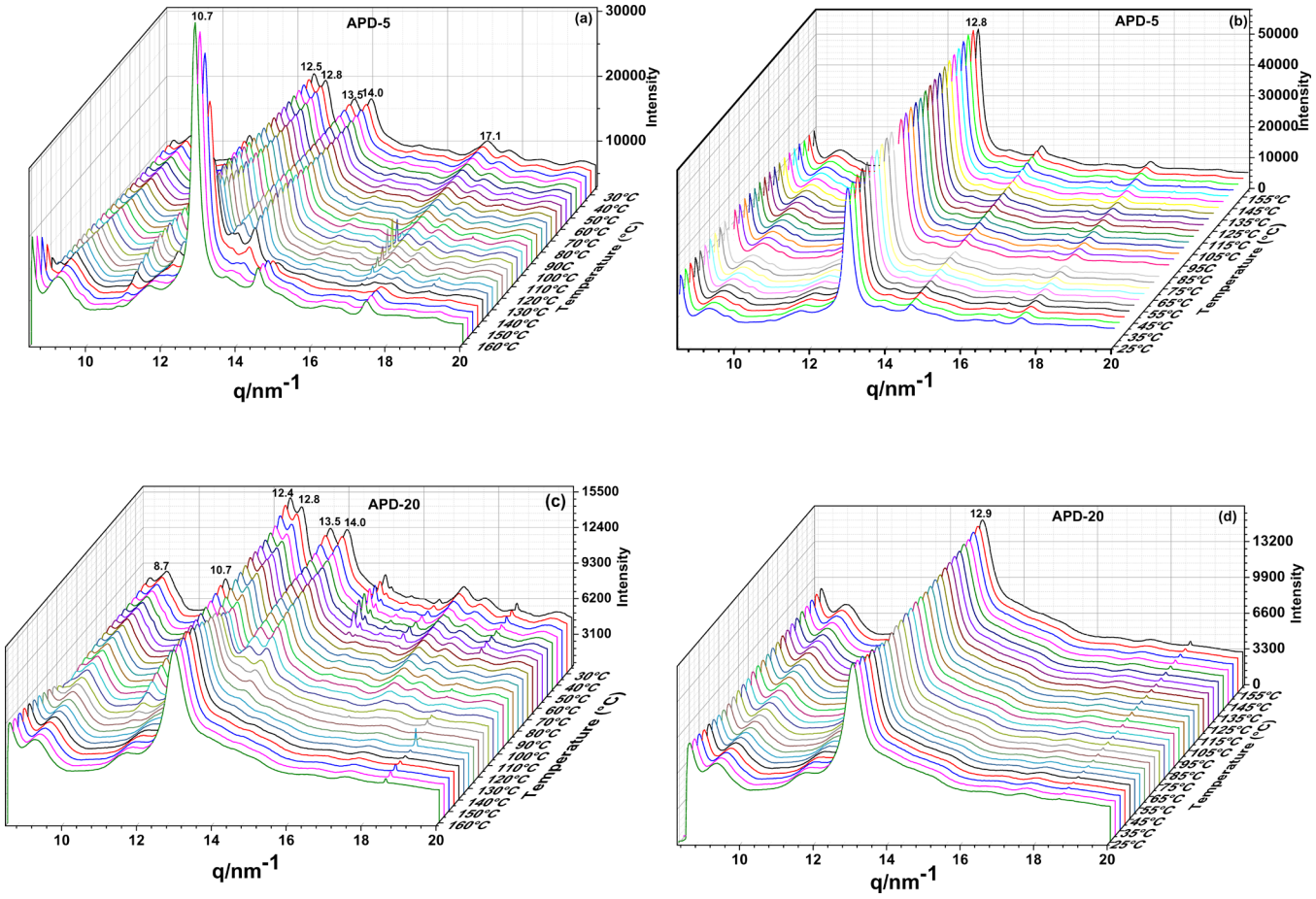

Figure 5. WAXS profile of (a,b) APD-5 and (c,d) APD-20 as a function of temperature recorded during heating (a,c) and cooling (b,d) of the complex from 25 to 160 °C and vice versa, respectively.

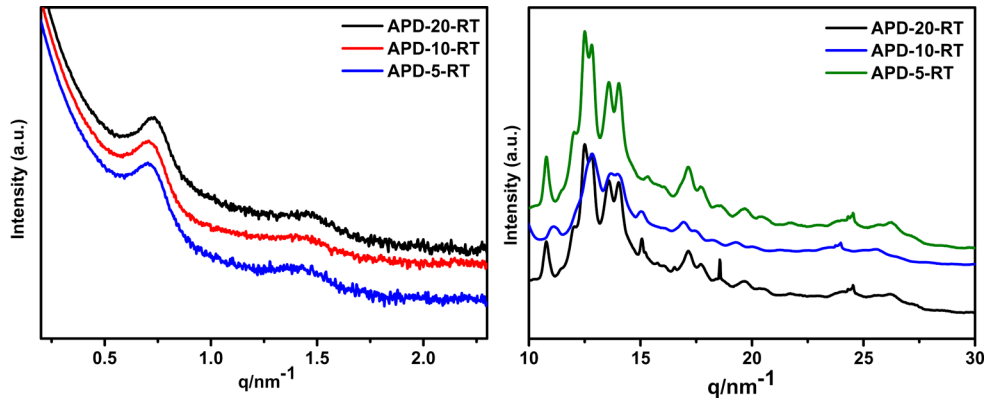

Figure 6. (a) SAXS and (b) WAXS patterns at room temperature of APD-5, APD-10, and APD-20 (curves are offset for clarity).

stability of the complex at higher concentrations of PDP. The crystalline structure and periodic organization of the complexes as a function of temperature were analyzed by SAXS and WAXS. Two different crystal structures of inclusion complexes were revealed by WAXS.

The complexation of PDP with amylose is a promising approach to improve the utilization of these kinds of complexes in food and drug industries, for instance, nanoencapsulation, controlled release of the drugs, and flavor encapsulations. In addition, the self-assembly of the inclusion complexes is expected to have potential applications in supramolecular chemistry for the fabrication of hierarchical morphologies, such as phase compatibilizers.

AUTHOR INFORMATION

Corresponding Authors

*E-mail: kamlesh.kumar@csio.res.in, kksaini@gmail.com (K.K).

*E-mail: k.u.loos@rug.nl (K.L.).

ORCID

Katja Loos: 0000-0002-4613-1159

DOI: 10.1021/acsomega.9b02388
ACS Omega 2019, 4, 17807−17813

Present Address

[#]Present address: Ubiquitous Analytical Techniques, CSIR-Central Scientific Instruments Organisation, Sector-30, Chandigarh 160030, India

Notes

The authors declare no competing financial interest.

■ ACKNOWLEDGMENTS

This research was funded by a VIDI research grant from the Netherlands Organization for Scientific Research (NWO). Measurements of SAXS and WAXS were performed on the DUBBLE beamline of ESRF Grenoble, France, and the authors are very grateful to Wim Bras, Giuseppe Portale, and Daniel Hermida-Merino for experimental assistance.

■ REFERENCES

(1) Semeijn, C.; Buwalda, P. L., Chapter 9 - Potato Starch. In *Starch in Food* (Second Edition), Sjöö, M.; Nilsson, L., Eds. Woodhead Publishing: 2018; pp 353−372.
(2) Jane, J. Starch Properties, Modifications, and Applications. *J. Macromol. Sci., Part A: Pure Appl. Chem.* **1995**, *32*, 751−757.
(3) Singh, J.; Kaur, L.; McCarthy, O. J. Factors influencing the physico-chemical, morphological, thermal and rheological properties of some chemically modified starches for food applications—A review. *Food Hydrocolloids* **2007**, *21*, 1−22.
(4) Kumar, K.; Woortman, A. J. J.; Loos, K. Synthesis of amylose-b-P2VP block copolymers. *Macromol. Rapid Commun.* **2015**, *36*, 2097−2101.
(5) Kumar, K.; Boonstra, M.; Loos, K. Synthesis of carbon microrings using polymer blends as templates. *RSC Adv.* **2015**, *5*, 33294−33298.
(6) Rachmawati, R.; Woortman, A. J. J.; Kumar, K.; Loos, K. Inclusion complexes between polytetrahydrofuran-b-amylose block copolymers and polytetrahydrofuran chains. *Macromol. Biosci.* **2015**, *15*, 812−828.
(7) Kumar, K.; Woortman, A. J. J.; Loos, K. Synthesis of amylose−polystyrene inclusion complexes by a facile preparation route. *Biomacromolecules* **2013**, *14*, 1955−1960.
(8) Putseys, J. A.; Lamberts, L.; Delcour, J. A. Amylose-inclusion complexes: Formation, identity and physico-chemical properties. *J. Cereal Sci.* **2010**, *51*, 238−247.
(9) Kim, O.-K.; Choi, L. S. Supramolecular Inclusion Complexation of Amylose with Photoreactive Dyes. *Langmuir* **1994**, *10*, 2842−2846.
(10) Park, B.; Appell, M. *Advances in Applied Nanotechnology for Agriculture*. American Chemical Society: 2013; Vol. *1143*, p 0.
(11) Rodríguez, S. D.; Bernik, D. L.; Méreau, R.; Castet, F.; Champagne, B.; Botek, E. Amylose−Vanillin Complexation Assessed by a Joint Experimental and Theoretical Analysis. *J. Phys. Chem. C* **2011**, *115*, 23315−23322.
(12) Heinemann, C.; Conde-Petit, B.; Nuessli, J.; Escher, F. Evidence of Starch Inclusion Complexation with Lactones. *J. Agric. Food Chem.* **2001**, *49*, 1370−1376.
(13) Kaneko, Y.; Saito, Y.; Nakaya, A.; Kadokawa, J.-i.; Tagaya, H. Preparation of inclusion complexes composed of amylose and strongly hydrophobic polyesters in parallel enzymatic polymerization system. *Macromolecules* **2008**, *41*, 5665−5670.
(14) Kadokawa, J.-i.; Kaneko, Y.; Tagaya, H.; Chiba, K. Synthesis of an amylose−polymer inclusion complex by enzymatic polymerization of glucose 1-phosphate catalyzed by phosphorylase enzyme in the presence of polyTHF: a new method for synthesis of polymer−polymer inclusion complexes. *Chem. Commun.* **2001**, 449−450.
(15) Kida, T.; Minabe, T.; Okabe, S.; Akashi, M. Partially-methylated amyloses as effective hosts for inclusion complex formation with polymeric guests. *Chem. Commun.* **2007**, 1559−1561.
(16) Tufvesson, F.; Wahlgren, M.; Eliasson, A.-C. Formation of Amylose-Lipid Complexes and Effects of Temperature Treatment. Part 1. Monoglycerides. *Starch - Stärke* **2003**, *55*, 61−71.
(17) Gelders, G. G.; Goesaert, H.; Delcour, J. A. Amylose−Lipid Complexes as Controlled Lipid Release Agents during Starch Gelatinization and Pasting. *J. Agric. Food Chem.* **2006**, *54*, 1493−1499.
(18) Zabar, S.; Lesmes, U.; Katz, I.; Shimoni, E.; Bianco-Peled, H. Studying different dimensions of amylose−long chain fatty acid complexes: Molecular, nano and micro level characteristics. *Food Hydrocolloids* **2009**, *23*, 1918−1925.
(19) Lesmes, U.; Barchechath, J.; Shimoni, E. Continuous dual feed homogenization for the production of starch inclusion complexes for controlled release of nutrients. *Innovative Food Sci. Emerging Technol.* **2008**, *9*, 507−515.
(20) Heinemann, C.; Zinsli, M.; Renggli, A.; Escher, F.; Conde-Petit, B. Influence of amylose-flavor complexation on build-up and breakdown of starch structures in aqueous food model systems. *LWT - Food Sci. Technol.* **2005**, *38*, 885−894.
(21) Whittam, M. A.; Orford, P. D.; Ring, S. G.; Clark, S. A.; Parker, M. L.; Cairns, P.; Miles, M. J. Aqueous dissolution of crystalline and amorphous amylose-alcohol complexes. *Int. J. Biol. Macromol.* **1989**, *11*, 339−344.
(22) Takeo, K. I.; Kuge, T. Complexes of Starchy Materials with Organic Compounds: Part III. X-Ray Studies on Amylose and Cyclodextrin Complexes. *Agric. Biol. Chem.* **1969**, *33*, 1174−1180.
(23) Yamashita, Y.; Monobe, K. Single crystals of amylose V complexes. III. Crystals with 81 helical configuration. *J. Polym. Sci., Part A-2* **1971**, *9*, 1471−1481.
(24) Lochab, B.; Shukla, S.; Varma, I. K. Naturally occurring phenolic sources: monomers and polymers. *RSC Adv.* **2014**, *4*, 21712−21752.
(25) Bras, W.; Dolbnya, I. P.; Detollenaere, D.; van Tol, R.; Malfois, M.; Greaves, G. N.; Ryan, A. J.; Heeley, E. Recent experiments on a small-angle/wide-angle X-ray scattering beam line at the ESRF. *J. Appl. Crystallogr.* **2003**, *36*, 791−794.
(26) Nikonenko, N. A.; Buslov, D. K.; Sushko, N. I.; Zhbankov, R. G. Investigation of stretching vibrations of glycosidic linkages in disaccharides and polysaccarides with use of IR spectra deconvolution. *Biopolymers* **2000**, *57*, 257−262.
(27) Bernazzani, P.; Chapados, C.; Delmas, G. Double-helical network in amylose as seen by slow calorimetry and FTIR. *J. Polym. Sci., Part B: Polym. Phys.* **2000**, *38*, 1662−1677.
(28) Aburto, J.; Alric, I.; Thiebaud, S.; Borredon, E.; Bikiaris, D.; Prinos, J.; Panayiotou, C. Synthesis, characterization, and biodegradability of fatty-acid esters of amylose and starch. *J. Appl. Polym. Sci.* **1999**, *74*, 1440−1451.
(29) Eichhorn, K.-J.; Fahmi, A.; Adam, G.; Stamm, M. Temperature-dependent FTIR spectroscopic studies of hydrogen bonding of the copolymer poly (styrene-b-4-vinylpyridine) with pentadecylphenol. *J. Mol. Struct.* **2003**, *661-662*, 161−170.
(30) Rodríguez, S. D.; Bernik, D. L. Host−Guest Molecular Interactions in Vanillin/Amylose Inclusion Complexes. *Appl. Spectrosc.* **2013**, *67*, 884−891.
(31) Yang, Y.; Gu, Z.; Zhang, G. Delivery of Bioactive Conjugated Linoleic Acid with Self-Assembled Amylose−CLA Complex. *J. Agric. Food Chem.* **2009**, *57*, 7125−7130.
(32) Rachmawati, R.; Woortman, A. J. J.; Loos, K. Facile Preparation Method for Inclusion Complexes between Amylose and Polytetrahydrofurans. *Biomacromolecules* **2013**, *14*, 575−583.
(33) Kuang, Q.; Xu, J.; Liang, Y.; Xie, F.; Tian, F.; Zhou, S.; Liu, X. Lamellar structure change of waxy corn starch during gelatinization by time-resolved synchrotron SAXS. *Food hydrocolloids* **2017**, *62*, 43−48.
(34) Biais, B.; Le Bail, P.; Robert, P.; Pontoire, B.; Buléon, A. Structural and stoichiometric studies of complexes between aroma compounds and amylose. Polymorphic transitions and quantification in amorphous and crystalline areas. *Carbohydr. Polym.* **2006**, *66*, 306−315.
(35) Blazek, J.; Gilbert, E. P. Application of small-angle X-ray and neutron scattering techniques to the characterisation of starch structure: A review. *Carbohydr. Polym.* **2011**, *85*, 281−293.
(36) Helbert, W.; Chanzy, H. Single crystals of V amylose complexed with n-butanol or n-pentanol: structural features and properties. *Int. J. Biol. Macromol.* **1994**, *16*, 207−213.

DOI: 10.1021/acsomega.9b02388
ACS Omega 2019, 4, 17807−17813

(37) Takeo, K.; Tokumura, A.; Kuge, T. Complexes of Starch and its Related Materials with Organic Compounds. Part. X. X-Ray Diffraction of Amylose-Fatty Acid Complexes. *Starch - Stärke* **1973**, *25*, 357−362.
(38) Feng, T.; Wang, H.; Wang, K.; Liu, Y.; Rong, Z.; Ye, R.; Zhuang, H.; Xu, Z.; Sun, M. Preparation and structural characterization of different amylose−flavor molecular inclusion complexes. *Starch - Stärke* **2018**, *70*, 1700101.
(39) Derycke, V.; Vandeputte, G. E.; Vermeylen, R.; De Man, W.; Goderis, B.; Koch, M. H. J.; Delcour, J. A. Starch gelatinization and amylose−lipid interactions during rice parboiling investigated by temperature resolved wide angle X-ray scattering and differential scanning calorimetry. *J. Cereal Sci.* **2005**, *42*, 334−343.
(40) Le Bail, P.; Bizot, H.; Ollivon, M.; Keller, G.; Bourgaux, C.; Buléon, A. Monitoring the crystallization of amylose−lipid complexes during maize starch melting by synchrotron x-ray diffraction. *Biopolymers* **1999**, *50*, 99−110.
(41) Yang, Z.; Gu, Q.; Hemar, Y. In situ study of maize starch gelatinization under ultra-high hydrostatic pressure using X-ray diffraction. *Carbohydr. Polym.* **2013**, *97*, 235−238.
(42) Le Bail, P.; Bizot, H.; Buléon, A. 'B' to 'A' type phase transition in short amylose chains. *Carbohydr. Polym.* **1993**, *21*, 99−104.
(43) Li, W.; Shan, Y.; Xiao, X.; Luo, Q.; Zheng, J.; Ouyang, S.; Zhang, G. Physicochemical Properties of A- and B-Starch Granules Isolated from Hard Red and Soft Red Winter Wheat. *J. Agric. Food Chem.* **2013**, *61*, 6477−6484.
(44) Biliaderis, C. G.; Page, C. M.; Maurice, T. J. Non-equilibrium melting of amylose-V complexes. *Carbohydr. Polym.* **1986**, *6*, 269−288.
(45) Nakazawa, Y.; Wang, Y.-J. Effect of annealing on starch−palmitic acid interaction. *Carbohydr. Polym.* **2004**, *57*, 327−335.
(46) Obiro, W. C.; Sinha Ray, S.; Emmambux, M. N. V-amylose structural characteristics, methods of preparation, significance, and potential applications. *Food Rev. Int.* **2012**, *28*, 412−438.
(47) Tu, C.-W.; Kuo, S.-W.; Chang, F.-C. Supramolecular self-assembly through inclusion complex formation between poly(ethylene oxide-b-N-isopropylacrylamide) block copolymer and α-cyclodextrin. *Polymer* **2009**, *50*, 2958−2966.

DOI: 10.1021/acsomega.9b02388
ACS Omega 2019, 4, 17807−17813